Abscissic acid specific expression of *RAB18* involves activation of anion channels in *Arabidopsis thaliana* suspension cells

Thanos Ghelis[a,1], Olivier Dellis[a,b,1], Emmanuelle Jeannette[a,*], Françoise Bardat[a], Daniel Cornel[b], Emile Miginiac[a], Jean-Pierre Rona[b], Bruno Sotta[a]

[a] *Physiologie Cellulaire et Moléculaire des Plantes, UMR CNRS 7632, case 156, Université Pierre et Marie Curie (Paris VI), 4 place Jussieu, 75252 Paris Cedex 05, France*

[b] *Electrophysiologie des Membranes, LPCMSP, case 7069, Université Denis Diderot (Paris VII), 2 place Jussieu, 75221 Paris Cedex 05, France*

Received 21 March 2000; received in revised form 25 April 2000

Edited by Ulf-Ingo Flügge

Abstract The abscissic acid (ABA) transduction cascade following the plasmalemma perception was analyzed in intact *Arabidopsis thaliana* suspension cells. In response to impermeant ABA, anion currents were activated and K^+ inward rectifying currents were inhibited. Anion current activation was required for the ABA specific expression of *RAB18*. By contrast, specific inhibition of K^+ channels by tetraethylammonium or Ba^{2+} did not affect *RAB18* expression. Thus, outer plasmalemma ABA perception triggered two separated signaling pathways.

Key words: Abscissic acid perception; Anion current; K^+ inward rectifying current; *RAB18*; *Arabidopsis thaliana* suspension cell

1. Introduction

The plant hormone abscissic acid (ABA) triggers numerous physiological responses like the maturation and dormancy of seeds, accumulation of reserves and adaptation to environmental stresses. ABA also plays a major role in the regulation of transpiration via control of stomatal closure [1]. This physiological response has become the most important in the study of the mechanisms of ABA perception and transduction in cells [2,3]. Many studies emphasize the prominent role of ionic fluxes in the control of stomatal closure induced by ABA. Rapid and slow depolarization-induced anion channels have been shown in guard cells [4,5]. They contribute to initiate plasmalemma depolarization and to induce long-term anion efflux controlling the maintenance of low plasma membrane potentials [4]. The consequence is an activation of voltage-dependent K^+ outward rectifying currents (K^+ORC) and stomatal closure [6].

Besides stomatal closure which is due to fast ionic movements, ABA induces the expression of numerous genes, most of them related to the maturation of seeds and desiccation tolerance [7]. The control of the expression of these ABA-inducible genes shows some common features with that of stomatal closure. For instance, protein kinases, protein phosphatases and phospholipases C and D have been involved in the ABA transduction cascade [8,9]. However, a few experimental models are suitable for studying the relationships between ABA perception, ionic movements and gene expression.

In de-differentiated *Arabidopsis thaliana* suspension cells, ABA-binding plasmalemma proteins were detected by means of ABA–protein conjugates used as affinity probes [10]. The same impermeant conjugates allowed us to demonstrate the existence of external plasma membrane perception of ABA in these intact cells. Extracellular perception of ABA induced a fast membrane depolarization, followed with the activation of K^+ORC and then induction of the specific ABA-inducible *RAB18* gene [11]. Hence, *A. thaliana* suspension cells constitute a handy model convenient for studying the complex network of ABA signal transduction. In this paper we demonstrate that the activity of anion channels, but not K^+ channels, is part of the signaling cascade necessary for *RAB18* expression.

2. Materials and methods

2.1. Plant material

A. thaliana L. ec. Columbia cells were obtained by Axelos et al. [12]. They were cultured at 24°C, under continuous white light (40 μE m^{-2} s^{-1}) with an orbital agitation at 130 rpm, in 500 ml Erlenmeyer flasks containing 200 ml Jouanneau and Péaud-Lenoël culture medium [13]. Subculture (1/10 dilution) was done weekly and the experiments were conducted on 4-day-old cells after subculture. The pH of the culture medium was 6.8. The viability of the cells during the experimental time course was systematically checked with Trypan blue tests (not shown).

Arabidopsis protoplasts were isolated after 3 h digestion of suspension cells in fresh culture medium supplemented by 0.66% Cellulase R10 (Onozuka, Japan), 0.2% Caylase M3 (Cayla, France) and 140 g/l sucrose. The protoplast suspension was then collected after filtration on 40 μm mesh and rinsed twice with fresh culture medium supplemented with 140 g/l sucrose.

2.2. RAB18 responsive test and Northern blot analysis

A 5 ml suspension was incubated for 3 h under the conditions of culture. ABA–bovine serum albumin (BSA) purified conjugate (10^{-5} M equivalent ABA) was added in 50 mM Na_2SO_4, 50 mM pH 6.8 phosphate buffer. All the channel blockers were added with ABA–BSA simultaneously. Northern blot analyses were performed according to the protocol previously described [11].

2.3. Electrophysiology

The cells were equilibrated for 24 h before voltage-clamp electrophysiological experiments in fresh culture medium (20 mM KNO_3, 0.9 mM $CaCl_2$, 0.45 mM $MgSO_4$, pH 6.8). Voltage-clamp measurements of whole-cell currents from intact cells were carried out at room temperature (20–22°C) using the technique of the discontinuous single voltage-clamp microelectrode [11,14]. Microelectrode tips were of 0.5 μm diameter, they were filled with 600 mM KCl and had electrical resistances from 50 to 80 MΩ. Channel inhibitors and ABA–BSA

*Corresponding author. Fax: (33)-1-44276232.
E-mail: ema@ccr.jussieu.fr

[1] These authors have equally contributed to this work.

PII: S0014-5793(00)01574-X

were diluted in the bathing medium. In whole-cell current measurements the membrane potential was held at −40 mV. Two voltage protocols were used to study the inward currents. The first one was obtained by hyperpolarizing pulses from −200 to −40 (Fig. 1) or 0 mV (Fig. 5). In the other one, used to show anion currents [4], currents were activated by a depolarizing prepulse (+100 mV for 4.5 s), then hyperpolarizing pulses ranging from −200 to 0 mV in 40 mV steps for 9.5 s (Fig. 4). We systematically checked that cells were correctly clamped by comparing the protocol voltage values with those really imposed.

For patch-clamp recordings, the external bath solution contained in mM: KCl 100, $MgCl_2$ 1, $CaCl_2$ 1, HEPES 5, pH 7 adjusted with Tris and 500 mOsm/kg with sucrose. ABA–BSA was diluted in the bathing medium. Glass pipettes (Kimax GC150F) were filled with a solution containing in mM: K-glutamate 100, HEPES 10, $MgCl_2$ 2, EGTA 2, MgATP 2, pH 7.2 adjusted with Tris and 520 mOsm/kg with sucrose. Their electrical resistance ranged from 5 to 10 MΩ. Experiments were carried out using the whole-cell recording mode of patch-clamp [15]. Current records were carried out at room temperature (20–25°C). Seal resistances were >800 MΩ. Cell and pipette capacitances were compensated by the patch-clamp amplifier AxoPatch 1D (Axon Instruments). Whole-cell currents were acquired on computer (IPC 386) with pClamp 6.0 software (Axon Instruments) and leak currents were subtracted. To enhance inward K^+ currents, protoplasts were held at +100 mV and then eight pulses from −200 to −80 mV in 20 mV steps were applied for 5 s.

3. Results

3.1. *A. thaliana* suspension cells exhibit inward currents

Whole-cell inward currents were characterized in *A. thaliana* suspension intact cells with the voltage-clamp technique. The membrane potential (E_m) was −42 ± 9.5 mV ($n = 132$) in the fresh culture medium. This value is close to the E_K (−40.5 mV; see [11]) calculated with the Nernst equation. Following negative pulses (−200 to −40 mV) three types of inward rectifying current (IRC) patterns were distinguished (Fig. 1). Most of the cells (71%) exhibited IRC mediated by an anion efflux (Fig. 1a, confirmed by Zn^{2+} and 9-AC treatments and illustrated below in Fig. 4). Eighteen percent of the cells showed a typical K^+ IRC pattern (Fig. 1b, confirmed by tetraethylammonium (TEA) treatment and illustrated below in Fig. 3) and 11% a more complex IRC pattern (Fig. 1c). The intensity of typical K^+ IRCs was low compared to that of other IRCs recorded.

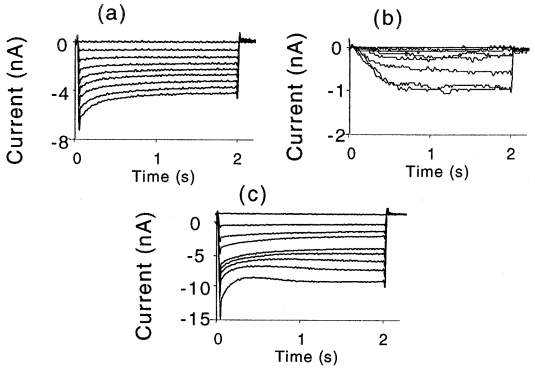

Fig. 1. Intact *A. thaliana* suspension cells exhibit three distinct patterns of whole-cell IRC. Currents were recorded on 4-day-old cells in fresh culture medium ($n = 132$). Plasma membrane currents resulting from hyperpolarizing voltage pulses from −200 to −40 mV for 2 s (in 20 mV steps). The holding potential was −40 mV. a: 71% of the cells exhibit a typical anion-like current pattern. The diameter of the cell studied in this example was 42 μm. b: Whole-cell K^+ IRC were also well-resolved in 11% of the cells. The diameter of the cell studied in this example was 38 μm. c: 18% of the cells show a complex inward current pattern. The diameter of the cell studied in this example was 30 μm.

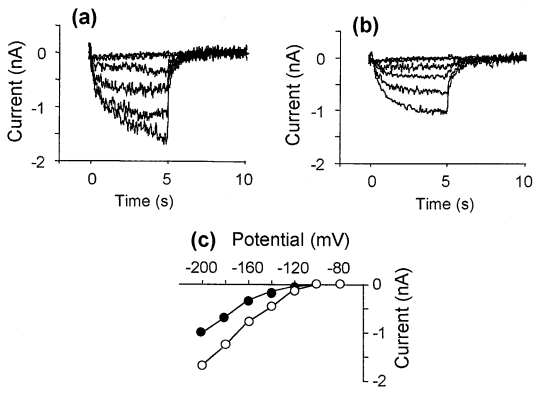

Fig. 2. Effect of ABA–BSA on the whole-cell K^+ IRC measured across the plasma membrane of *A. thaliana* suspension cell protoplasts. Protoplast currents were recorded by applying seven pulses from −200 to −80 mV in 20 mV-steps. Holding potential was +100 mV. a: Control before addition of ABA–BSA. b: 20 min after adding ABA–BSA at 10^{-5} M equivalent ABA. c: Current–voltage relationship of K^+ IRC measured at 4.95 s before (dark circles) and after (open circles) addition of ABA–BSA for 20 min. The diameter of protoplasts was 35–40 μm. These data are representative of three experiments.

3.2. Outward perception of ABA inhibits K^+ IRC

Characterization of K^+ IRC was done by whole-cell patch-clamp analysis in protoplasts prepared from *A. thaliana* cells. K^+ IRC were present in six out of 29 tested protoplasts. K^+

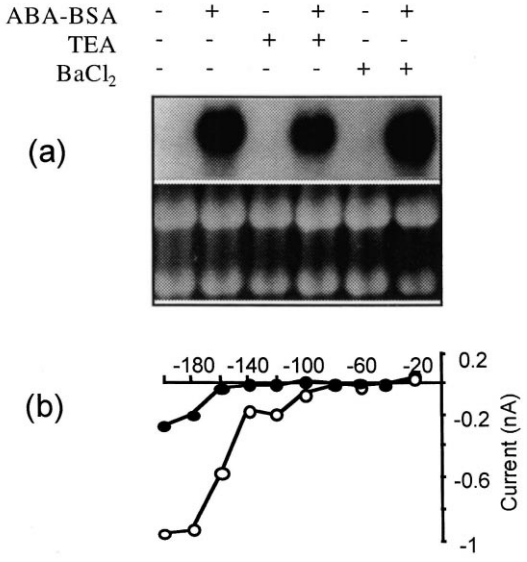

Fig. 3. Induction of *RAB18* gene expression triggered by an extracellular ABA perception is independent of K^+ channel activities in *A. thaliana* suspension cells. a: Northern blot analysis of total RNA (10 μg) from cells incubated simultaneously for 3 h with ABA–BSA conjugate (10^{-5} M equivalent ABA) and TEA-Cl (10 mM) or $BaCl_2$ (10 mM). Ethidium bromide staining of rRNAs is shown as control. b: Current–voltage relationship of K^+ inward currents recorded before (dark circles) and after (open circles) TEA-Cl (10 mM) adding. Plasma membrane currents resulting from voltage pulses from −200 to −20 mV (in 20 mV steps for 2 s). Holding potential was −40 mV. The diameter of the cell was 42 μm.

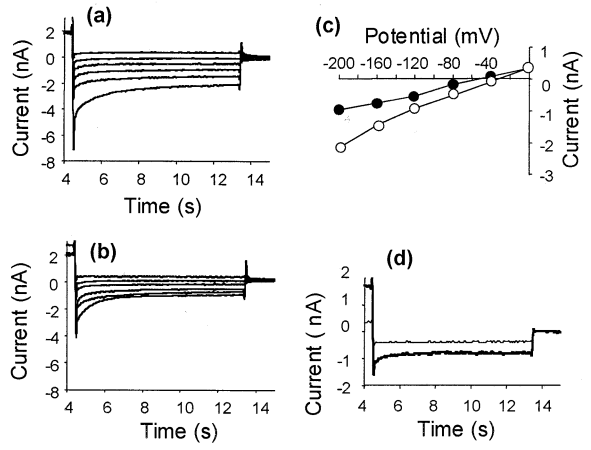

Fig. 4. Pharmacological characterization of plasma membrane anion currents of intact *A. thaliana* suspension cells. Currents were activated by a depolarizing prepulse (+100 mV for 4.5 s) followed with 9 s hyperpolarizing pulses ranging from −200 to 0 mV (in 40 mV steps). Holding potential was −40 mV. Only the final 250 ms of the 4.5 s prepulse are shown. a: Control. b: 3 min after 200 μM 9-AC. c: Current–voltage relationship of inward currents recorded before (dark circles) and after (open circles) 9-AC adding. Current–voltage relationship determined from currents recorded at 13.5 s. The diameter of the cell was 40 μm. This experiment is representative of 5 replications. d: Currents recorded under −200 mV pulse before (bold line) and 3 min after (standard line) adding of 1 mM $ZnSO_4$. Currents were measured in the culture medium supplemented with TEA-NO_3 10 mM and $BaCl_2$ 10 mM. The diameter of the cell was 42 μm. This experiment is representative of eight replications.

IRC were clamped for potential pulses within the range of −200 to −80 mV but they were detected only for pulses lower than −120 mV (Fig. 2). During the 5 s of pulse, K^+ IRC were not totally activated at −200 mV in controls (Fig. 2a) whereas activation occurred in ABA–BSA treated protoplasts (Fig. 2b). Adding ABA–BSA (Fig. 2c) to the bath solution, at 10^{-5} M for 20 min, decreased K^+ IRC intensity by 36 ± 4% ($n = 3$) at −200 mV.

3.3. *RAB18* expression is independent of the activity of K^+ channels

Impermeant ABA–BSA conjugate triggers the ABA specific expression of *RAB18*. When specific K^+ channel blockers were added with ABA–BSA simultaneously the level of *RAB18* transcripts was unchanged. Neither 10 mM TEA-Cl nor 10 mM $BaCl_2$ modified *RAB18* expression (Fig. 3a). The inhibition of K^+ IRC by TEA is illustrated in Fig. 3b. Thus, the activity of the K^+IRC channels is not a step of the ABA pathway leading to *RAB18* expression.

3.4. Impermeant ABA activates anion currents

The characterization of anion currents detected in the majority of the cells was carried out (Fig. 4). During the pulse, a two-step voltage-dependent deactivation was recorded with a quick phase (about 0.5 s) followed by a slower phase (about 8 s). This current exhibited the principal hallmarks of the slow relaxation currents of S-type *Arabidopsis* guard cell anion channels [16,17]. Pharmacological studies were performed to more precisely characterize these anion currents. Anion currents were partially inhibited with 200 μM 9-AC (37 ± 9.5% at −200 mV) in five out of the eight cells studied (Fig. 4a–c). Zinc ions (1 mM $ZnSO_4$) also partially reduced the deactivation currents in eight out of the 12 cells studied: at 9.5 s, the inhibition was 51 ± 10% at −200 mV (Fig. 4d). Hence, voltage-dependent anion currents were actually detected in the majority of the *A. thaliana* suspension cells.

ABA–BSA activates anion currents (Fig. 5). An increase in anion current intensities was recorded (38 ± 10% at 500 ms for −200 mV) after 1 min of 10^{-5} M ABA–BSA application (Fig. 5a–c, representative of five out of eight cells). Control cells treated with BSA alone exhibited no activation of anion currents (not illustrated). Treatment with ABA–BSA induced a depolarization shown by the shift (8 mV) of the resting membrane potential (Fig. 5c). Zn^{2+} and 9-AC inhibited the ABA–BSA induced currents in a similar way as illustrated in Fig. 4. Therefore, outward perception of ABA stimulates the activity of voltage-dependent anion channels.

3.5. The activity of anion channels is necessary to induce *RAB18* expression

The anion channel blockers, $ZnSO_4$ and 9-AC, experimented in electrophysiological tests, were used to assess the role of anion channels in the ABA transduction cascade leading to *RAB18* expression. The viability of the cells during the 3 h experiment was systematically checked with Trypan blue tests (not shown). Controls show that inhibitors were unable to induce *RAB18* expression. Adding anion channel blockers with ABA–BSA inhibited the ABA-induced *RAB18* expression (Fig. 6). This inhibition was dose-dependent, from 100 to 500 μM for 9-AC and from 0.12 to 1 mM for $ZnSO_4$. Niflumic acid and 5-nitro-2-(3-phenylpropylamino)benzoic acid (NPPB), other anion channel blockers, were also efficient, from 125 to 500 μM for niflumic acid and 25 μM for NPPB, to inhibit ABA-induced *RAB18* expression (Fig. 6). Hence, when anion efflux was prevented, the *RAB18* transduction cascade was interrupted.

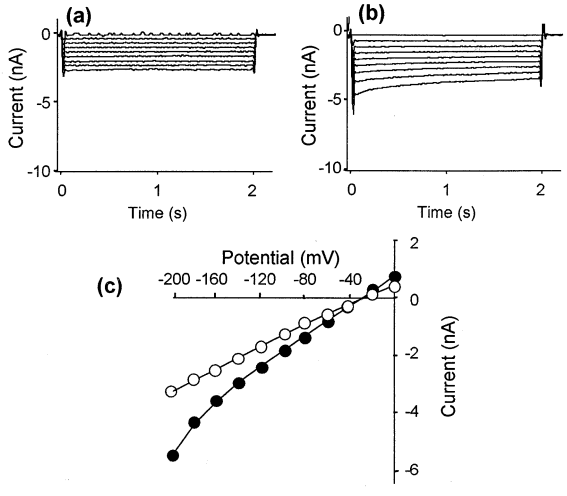

Fig. 5. Effect of ABA–BSA on the plasma membrane anion currents of intact *A. thaliana* suspension cells. Plasma membrane currents resulting from voltage pulses from −200 to 0 mV (in 20 mV steps for 2 s). Holding potential was −40 mV. a: Control before addition of ABA–BSA. b: One min after addition of extracellular 10^{-5} M ABA-BSA. c: Current–voltage relationship of inward currents is given before (dark circles) and after (open circles) addition of ABA–BSA. Current–voltage relationship determined from currents recorded at 1.9 s. The diameter of the cell was 38 μm. This experiment is representative of five replications.

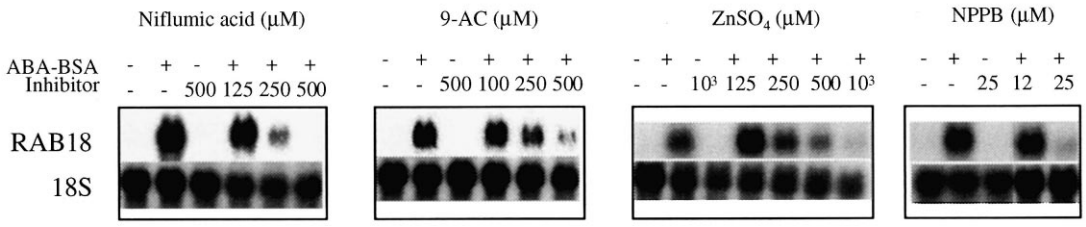

Fig. 6. Induction of *RAB18* gene expression triggered by an extracellular ABA perception is mediated by anion channel activity in *A. thaliana* suspension cells. Northern blot analysis of total RNA (10 μg) from cells incubated for 3 h with ABA–BSA conjugate at 10^{-5} M equivalent ABA and anion channels blockers (zinc, niflumic acid, 9-AC and NPPB) simultaneously. Similar RNA loading was checked by hybridization with an *Arabidopsis* 18S ribosomal cDNA probe.

4. Discussion

In *A. thaliana* suspension cells, ABA–BSA conjugate triggers a series of events: inhibition of K^+ IRC, activation of anion currents (present results), depolarization of the plasma membrane, activation of K^+ ORC and induction of *RAB18* gene expression [11].

Voltage-clamp experiments done in intact cells demonstrate that inward currents recorded were due to both anion efflux and K^+ influx (Fig. 1). The percentage of cells in which the anion current pattern was well resolved (i.e. 71%, Fig. 1a) is close to that reported by Schroeder and Keller [4] on *Vicia faba* guard cell protoplasts and by Thomine et al. [18] on epidermal protoplasts of *Arabidopsis* hypocotyls. The culture medium of the cells contains 20 mM KNO_3 and 0.9 mM $CaCl_2$. Due to the higher permeability of plasmalemma to NO_3^- than to Cl^- ($P_{NO_3^-}/P_{Cl^-} \approx 2.6$), the cells accumulate NO_3^- [19,20]. Thus, the anion currents recorded in suspension cells are probably due mainly to nitrate and not to chloride efflux.

Two distinct types of anion channels have been described in plants [4,5]. Rapid (R-type) and slow (S-type) anion channels contribute to initiate membrane depolarization, then to maintain low plasma membrane potentials in *V. faba* guard cells [4]. In *A. thaliana* suspension cells we did not distinguish R- or S-type anion channels (Fig. 4). However, an overall activation of anion currents was recorded within the experimental time-course (Fig. 4). The inhibitors tested confirmed the involvement of anion currents. However, blockers were less efficient in whole cells than with the excised patch-clamp technique focused on one single ion channel. For example, anion channel activities were not completely abolished with 200 μM 9-AC (40%) and 1 mM Zn^{2+} (50%) at −200 mV (Fig. 4). By contrast, higher inhibition values were reported in protoplasts of *V. faba* guard cells [21] or tobacco [22]. However, the partial inhibition observed with Zn^{2+} could also be due to the low effect of Zn^{2+} on S-type anion current activity, as already reported [23].

ABA activation of anion channels has been reported almost exclusively in guard cells. In *A. thaliana* [16,24,25], *V. faba* [26] and *Nicotiana benthamiana* [5], inhibitors of anion channels abolished the inhibition of stomatal opening induced by ABA. In *A. thaliana* suspension cells, we demonstrate also that anion channels are specifically activated by ABA–BSA conjugate. As evidenced by Northern blots issued from ABA-treated cells submitted to anion current inhibitors, the activity of anion channels is necessary for *RAB18* expression (Fig. 6). We obtained more similar data with free ABA (not illustrated) than with ABA–BSA. Thus, the outer-plasmalemma perception of ABA already observed [11] was confirmed in *A. thaliana* suspension cells. Our results are in accordance with observations reported by Anderson et al. [27] in *Commelina communis* guard cells and Schultz and Quatrano [28] in rice suspension cells. Data presented here are also in accord with data of Gilroy and Jones [29] in barley aleurone cells. However, since we did not try to inject ABA–BSA into the cells, our observations do not exclude an intracellular perception of the hormone which has been demonstrated by microinjections of caged ABA in *Commelina* guard cells [30].

Voltage-clamp experiments allowed the detection of typical K^+ IRC in 18% of the cells (Fig. 1b) and the participation of K^+ IRC to the overall inward current in 11% of the cells (Fig. 1c). Patch-clamp experiments were focused on K^+ IRC which were recorded in 20% of the protoplasts tested. These currents were sensitive to 10 mM TEA-Cl (Fig. 3b) as observed with channel proteins expressed from cloned K^+ IRC genes [31,32]. Intact cells and protoplasts of *A. thaliana* suspension cells exhibit similar K^+ IRC features to those described in guard cells [6], in xylem parenchyma cells [33] and in *Arabidopsis* suspension cells [34]. ABA inhibits about 50% of K^+ IRC intensity in protoplasts (Fig. 2) and in intact cells (not shown). The signals were noisy but comparable with those described in *V. faba* guard cells [35]. Nevertheless, it is noticeable that the opening and closure of K^+ IRC were slower in patch-clamp (Fig. 2) than in intact cell voltage-clamp experiments (Fig. 1b). Furthermore, in protoplasts, the ABA-induced inhibition of K^+ IRC was progressive and optimal inhibition was obtained within 20 min versus 1–2 min only in intact cells. The maximal effect of ABA on K^+ IRC inhibition in *V. faba* was also obtained in 20 min [36]. The fast response of intact *Arabidopsis* suspension cells leads us to question whether the preparation of protoplasts induced an alteration of the ABA receptors or whether the elimination of a cytosolic factor in the patch-clamp procedure occurred. TEA-Cl 10 mM inhibited both K^+ IRC (Fig. 3b) and K^+ ORC [11]. The same treatment with TEA-Cl (or with TEA-Br or TEA-NO_3, not shown), did not modify the expression of *RAB18* (Fig. 3a). Therefore, the ABA inhibition of K^+ IRC and activation of K^+ ORC are independent of *RAB18* expression.

A. thaliana suspension cells offer a convenient model to study ABA signaling with electrophysiological experiments coupled to the analysis of ABA-induced transcripts. In this model, the first element of ABA signal transduction that we detected was the activity of plasmalemma ion channels. *RAB18* expression is dependent on anion channel activity but independent of K^+ inward and outward channel activities.

Impermeant ABA–BSA conjugate mimicked the effect of free ABA. Thus, at least two transduction pathways triggered by ABA perception at the plasma membrane diverge after activation of anion channels. Once more, the importance of anion efflux is emphasized and constitutes an early major event detected in ABA signaling cascades [37]. In *A. thaliana* suspension cells, other elements of the ABA cascade should be studied. Anion channels are often activated by a previous increase in $[Ca^{2+}]_{cyt}$ [38,39]. Cytosolic calcium can modulate kinase-phosphatase activities [40] and activate phospholipases which produce second phospholipid messengers [41]. Thus, the role of Ca^{2+} and other second messengers in the ABA-induced *RAB18* expression will be analyzed.

Acknowledgements: We thank Dr. A. Vavasseur and Dr. F. Bouteau for helpful comments. We acknowledge Y. Habricot for technical assistance.

References

[1] Leung, J. and Giraudat, J. (1998) Annu. Rev. Plant Physiol. Plant Mol. Biol. 49, 199–222.
[2] Grill, E. and Himmelbach, A. (1998) Curr. Opin. Plant Biol. 1, 412–418.
[3] MacRobbie, E.A.C. (1998) Philos. Trans. R. Soc. Lond. B. Biol. Sci. 353, 1475–1488.
[4] Schroeder, J.I. and Keller, B.U. (1992) Proc. Natl. Acad. Sci. USA 89, 5025–5029.
[5] Grabov, A., Leung, J., Giraudat, J. and Blatt, M.R. (1997) Plant J. 12, 203–216.
[6] Blatt, M.R. (1990) Planta 180, 445–455.
[7] Campalans, A., Messeguer, R., Goday, A. and Pagès, M. (1999) Plant Physiol. Biochem. 37, 327–340.
[8] Jacob, T., Ritchie, S., Assmann, S.M. and Gilroy, S. (1999) Proc. Natl. Acad. Sci. USA 96, 12192–12197.
[9] Leung, J., Merlot, S. and Giraudat, J. (1997) Plant Cell 9, 759–771.
[10] Pédron, J., Brault, M., Näke, C. and Miginiac, E. (1998) Eur. J. Biochem. 252, 385–390.
[11] Jeannette, E., Rona, J.P., Bardat, F., Cornel, D., Sotta, B. and Miginiac, E. (1999) Plant J. 18, 13–22.
[12] Axelos, M., Curie, C., Mazzolini, L., Bardet, C. and Lescure, B. (1992) Plant Physiol. Biochem. 30, 123–128.
[13] Jouanneau, J.P. and Péaud-Lenoël, C. (1967) Physiol. Plant 20, 834–850.
[14] Bouteau, F., Dellis, O. and Rona, J.P. (1999) FEBS Lett. 458, 185–187.
[15] Hamill, O., Marty, A., Neher, E., Sakmann, B. and Sigworth, F.G. (1981) Pflügers Arch. Eur. J. Physiol. 391, 85–100.
[16] Forestier, C., Bouteau, F., Leonhardt, N. and Vavasseur, A. (1998) Pflügers Arch. Eur. J. Physiol. 436, 920–927.
[17] Pei, Z.M., Ghassemian, M., Kwak, C.M., McCourt, P. and Schroeder, J.I. (1998) Science 282, 287–290.
[18] Thomine, S., Guern, J. and Barbier-Brygoo, H. (1997) J. Membr. Biol. 159, 71–82.
[19] Frachisse, J.M., Thomine, S., Colcombet, J., Guern, J. and Barbier-Brygoo, H. (1999) Plant Physiol. 121, 253–261.
[20] Miller, A.J. and Smith, S.J. (1996) J. Exp. Bot. 47, 843–854.
[21] Marten, I., Zeilinger, C., Redhead, C., Landry, D.W., Al-Awqati, Q. and Hedrich, R. (1992) EMBO J. 11, 3569–3575.
[22] Zimmermann, S., Thomine, S., Guern, J. and Barbier-Brygoo, H. (1994) Plant J. 6, 707–716.
[23] Schroeder, J.I., Schmidt, C. and Sheaffer, J. (1993) Plant Cell 5, 1831–1841.
[24] Armstrong, F., Leung, J., Grabov, A., Brearley, J., Giraudat, J. and Blatt, M.R. (1995) Proc. Natl. Acad. Sci. USA 92, 9520–9524.
[25] Pei, Z.M., Kuchitsu, K., Ward, J.M., Schwarz, M. and Schroeder, J.I. (1997) Plant Cell 9, 409–423.
[26] Schwarz, M. and Schroeder, J. (1998) FEBS Lett. 428, 177–182.
[27] Anderson, B.E., Ward, J.M. and Schroeder, J.I. (1994) Plant Physiol. 104, 1177–1183.
[28] Schultz, T.F. and Quatrano, R.S. (1997) Plant Sci. 130, 63–71.
[29] Gilroy, S. and Jones, R. (1994) Plant Physiol. 104, 1185–1192.
[30] Allan, A.C., Fricker, M.D., Ward, J.L., Beale, M.H. and Trewavas, A.J. (1994) Plant Cell 6, 1319–1328.
[31] Schachtman, D.P., Schroeder, J.I., Lucas, W.J., Anderson, J.A. and Garber, R.F. (1992) Science 258, 1654–1658.
[32] Véry, A.A., Gaymard, F., Bosseux, C., Sentenac, H. and Thibaud, J.B. (1995) Plant J. 7, 321–332.
[33] Wegner, L.H., De Boer, A.H. and Raschke, K. (1994) J. Membr. Biol. 142, 363–379.
[34] Colombo, R. and Cerana, R. (1991) Plant Physiol. 97, 1130–1135.
[35] Lemtiri-Chlieh, F. and MacRobbie, E.A.C. (1994) J. Membr. Biol. 20, 951–962.
[36] Schwartz, A., Wei-Hua, W., Tucker, E.B. and Assmann, S.M. (1994) Proc. Natl. Acad. Sci. USA 91, 4019–4023.
[37] Barbier-Brygoo, H., Frachisse, J-M., Colcombet, J. and Thomine, S. (1999) Plant Physiol. Biochem. 37, 381–392.
[38] McAinsh, M.R. and Hetherington, A.M. (1998) Trends Plant Sci. 3, 32–36.
[39] Schroeder, J.I. and Hagiwara, S. (1989) Nature 338, 427–430.
[40] Sheen, J. (1996) Science 274, 1900–1902.
[41] Wang, X. (1999) Plant Physiol. 120, 645–651.